

Reduction in thermal boundary conductance due to proton implantation in silicon and sapphire

Patrick E. Hopkins, Khalid Hattar, Thomas Beechem, Jon F. Ihlefeld, Douglas L. Medlin et al.

Citation: *Appl. Phys. Lett.* **98**, 231901 (2011); doi: 10.1063/1.3592822

View online: <http://dx.doi.org/10.1063/1.3592822>

View Table of Contents: <http://apl.aip.org/resource/1/APPLAB/v98/i23>

Published by the [American Institute of Physics](http://www.aip.org).

Related Articles

Influence of isothermal hot pressing-doping treatment on the electrical and mechanical properties of bulk Bi-Sr-Ca-Cu-O

AIP Advances **2**, 042183 (2012)

Site preference of cation vacancies in Mn-doped Ga₂O₃ with defective spinel structure

Appl. Phys. Lett. **101**, 241906 (2012)

Low cost ion implantation technique

Appl. Phys. Lett. **101**, 224104 (2012)

Forward and back energy transfer between Cu²⁺ and Yb³⁺ in Ca_{1-x}CuSi₄O₁₀:Yb_x crystals

J. Appl. Phys. **112**, 093521 (2012)

Effects of DyHx and Dy₂O₃ powder addition on magnetic and microstructural properties of Nd-Fe-B sintered magnets

J. Appl. Phys. **112**, 093912 (2012)

Additional information on *Appl. Phys. Lett.*

Journal Homepage: <http://apl.aip.org/>

Journal Information: http://apl.aip.org/about/about_the_journal

Top downloads: http://apl.aip.org/features/most_downloaded

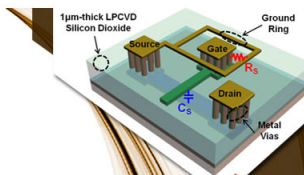
Information for Authors: <http://apl.aip.org/authors>

ADVERTISEMENT



**EXPLORE WHAT'S
NEW IN APL**

SUBMIT YOUR PAPER NOW!



SURFACES AND INTERFACES

Focusing on physical, chemical, biological, structural, optical, magnetic and electrical properties of surfaces and interfaces, and more...



ENERGY CONVERSION AND STORAGE

Focusing on all aspects of static and dynamic energy conversion, energy storage, photovoltaics, solar fuels, batteries, capacitors, thermoelectrics, and more...

Reduction in thermal boundary conductance due to proton implantation in silicon and sapphire

Patrick E. Hopkins,^{1,2,a)} Khalid Hattar,¹ Thomas Beechem,¹ Jon F. Ihlefeld,¹ Douglas L. Medlin,³ and Edward S. Piekos¹

¹Sandia National Laboratories, Albuquerque, New Mexico 87123, USA

²Department of Mechanical and Aerospace Engineering, University of Virginia, Charlottesville, Virginia 22904, USA

³Sandia National Laboratories, Livermore, California 87123, USA

(Received 24 March 2011; accepted 2 May 2011; published online 6 June 2011)

We measure the thermal boundary conductance across Al/Si and Al/Al₂O₃ interfaces that are subjected to varying doses of proton ion implantation with time domain thermoreflectance. The proton irradiation creates a major reduction in the thermal boundary conductance that is much greater than the corresponding decrease in the thermal conductivities of both the Si and Al₂O₃ substrates into which the ions were implanted. Specifically, the thermal boundary conductances decrease by over an order of magnitude, indicating that proton irradiation presents a unique method to systematically decrease the thermal boundary conductance at solid interfaces. © 2011 American Institute of Physics. [doi:10.1063/1.3592822]

The thermal transport across solid interfaces is a major inhibitor of heat flow in nanosystems.¹ Due to this fact, significant effort has focused on measurements to quantify and accompanying theory to describe thermal transmission across these boundaries. Most often, it is assumed that the solid interfaces are comprised of a perfectly abrupt or “flat” junction between two materials (see Refs. 1 and 2 for extensive reviews), whereas transport across nonideal interfaces are much less frequently considered. Despite this fact, several investigations have clearly shown that transport can be highly sensitive to the condition, or “flatness,” of these junctions. For example, Swartz and Pohl³ measured the thermal boundary conductance, h_K , across metallized sapphire interfaces with various degrees of surface damage, showing that surface damage affects h_K even at low temperature where phonon wavelengths are relatively long. Gundrum *et al.*⁴ came to this same conclusion for metal–metal interfaces by ion-bombarding the interfaces, showing that electron–electron interfacial scattering can be modified by the Kr dose. Hopkins *et al.*⁵ measured h_K across a series of Cr/Si interfaces with varying degrees of elemental mixing at the boundary finding that both electron–phonon scattering and phonon–phonon scattering in a so-called mixing region of Cr and Si caused a decrease in h_K .⁶ Recently, Collins and Chen⁷ found that the chemistry at diamond surfaces can affect h_K across Al/diamond interfaces and Hopkins *et al.*⁸ found that rms roughness at Si interfaces causes variations in h_K across Al/Si interfaces. From these studies, further investigation then seems warranted into “how” the imperfections around an interface influence h_K .

In response, we measure the thermal transport across Al/Si and Al/Al₂O₃ interfaces for a series of substrates that have been subjected to varying doses of proton implantation. After irradiation, we deposit Al films on the wafers and measure the thermal conductance across the interfaces with time domain thermoreflectance (TDTR). We find that the proton irradiation creates a major reduction in the thermal boundary

conductance. Specifically, the thermal boundary conductances decrease by over an order of magnitude, indicating that proton irradiation presents a unique method to systematically decrease the thermal boundary conductance at solid interfaces. Furthermore, by examining the varying degree to which h_K is reduced for each of the systems, the physical mechanisms driving this behavior are identified. This gives insight into the manner by which imperfections influence interfacial thermal transport.

To prepare the various interfaces, we implant four Si (001) and four Al₂O₃ (0001) samples with 300 keV protons at 1.2 μ A using a 400 keV implanter at the ion beam laboratory at Sandia National Laboratories in Albuquerque, NM. Areas of 0.36 cm² were implanted in a vacuum better than 10⁻⁷ Torr and at a dose rate of 5.79 \times 10¹³ ions cm⁻² s⁻¹ for times ranging from 10 to 10 000 s. The end of range of the protons were calculated using stopping and range of ions in matter (SRIM) to be 3.02 μ m with a scattering of 0.18 μ m in Si and 1.7 μ m with a scatter of 0.1 μ m in the sapphire.⁹ Based on these irradiation conditions, the total displacements per atom (dpa) was calculated to range from 7.19 \times 10⁻⁵ to 7.19 \times 10⁻² for the Si samples and between 3.56 \times 10⁻⁶ and 3.56 \times 10⁻³ for the Al₂O₃ samples, depending on the irradiation time.¹⁰ For equivalent irradiation times, the total dpa in Si was always calculated to be a factor of 2.02 greater than the total dpa in Al₂O₃ (i.e., for any irradiation exposure time, dpa_{Si}/dpa_{Al₂O₃}=2.02). Although some damage occurs throughout the irradiated region, the majority of the damage will be present in a band approximately the thickness of the straggle region centered on the end of range.¹¹ After ion implantation, we deposit 90 nm of Al on each of the samples. We also deposit 90 nm of Al on portions of the same Si and Al₂O₃ wafers that were not subjected to ion implantation (“as received”).

We measure h_K at the Al/Si and Al/Al₂O₃ interfaces with TDTR; typical experimental descriptions of TDTR and details of the thermal and lock-in analyses for thin-film systems are described elsewhere.^{12–14} We modulate the pump path at 11 MHz and monitor the ratio of the real to imaginary

^{a)}Electronic mail: phopkins@virginia.edu.

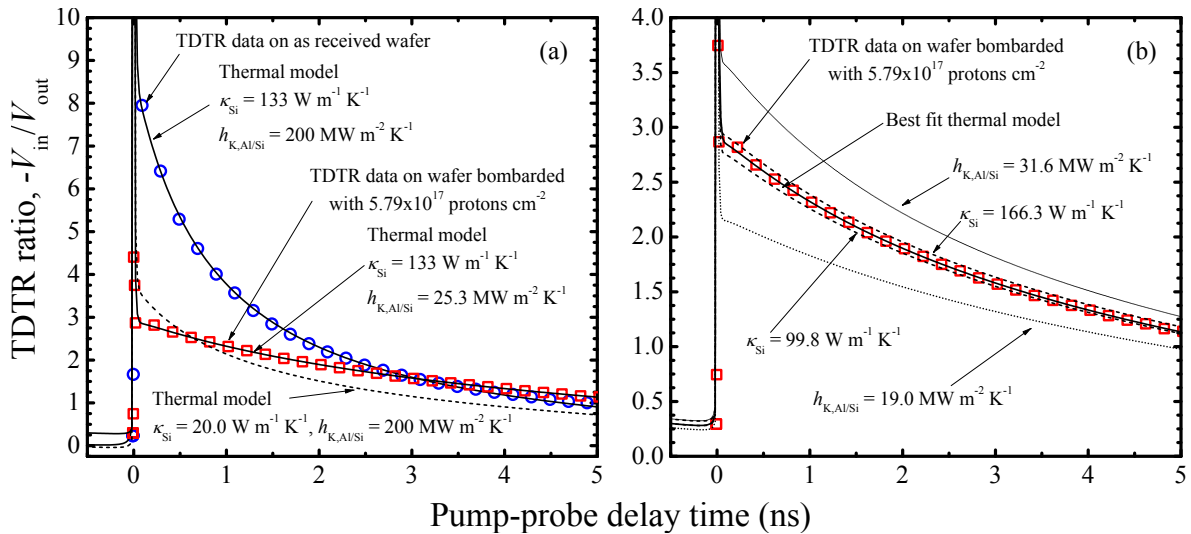


FIG. 1. (Color online) (a) Example of model fit to TDTR data on the as received Al/Si sample, and the Al/Si sample in which the Si substrate was subjected to ion dose of 5.79×10^{17} protons cm^{-2} . In the proton irradiated case, the model achieves a best fit to the data by only adjusting h_K . Adjusting κ results in a poor fit. (b) Sensitivity of the best fit model on the proton irradiated data in (a) to a $\pm 25\%$ change in κ or h_K .

signal of the probe beam ($-V_{\text{in}}/V_{\text{out}}$) locked into the pump frequency. For our analysis, we use bulk literature values for the heat capacity of each layer.¹⁵ We estimate the reduced thermal conductivity of the Al transducer layer from electrical resistivity measurements on the Al film,¹² although over the time domain of interest in this study, the TDTR analysis is minimally sensitive to the reduction in thermal conductivity of the Al film. We verify the thickness of the Al film with picosecond ultrasonics.^{16,17}

We fit our TDTR thermal model to the experimental data adjusting both the thermal boundary conductance, h_K , and the substrate thermal conductivity, κ . The measured thermal conductivities of the as received samples are within 10% of the literature values for bulk Si and Al_2O_3 . An example of the model fit to the data on the Al/Si as received sample is shown in Fig. 1(a). The thermal boundary conductances of as received samples are $h_K = 200 \text{ MW m}^{-2} \text{ K}^{-1}$ and $310 \text{ MW m}^{-2} \text{ K}^{-1}$ for the Al/Si and Al/ Al_2O_3 interfaces, respectively. These values are slightly higher than previous values reported in the literature,^{18–20} which could be due to processing conditions, surface preparation, and substrate quality.^{5,7,8,21} Our values for h_K at the Al/ Al_2O_3 as received interface is in good agreement with calculations of the diffuse mismatch model (DMM),²² where the DMM slightly over predicts the measurements at the Al/Si as received interface. We calculate the DMM for the Al/Si and Al/ Al_2O_3 interfaces as $250 \text{ MW m}^{-2} \text{ K}^{-1}$ and $305 \text{ MW m}^{-2} \text{ K}^{-1}$, respectively, using the procedure outlined by Duda *et al.*²³ We include optical phonons in these DMM calculations and we assume only two phonon elastic scattering at the interface.^{24,25} On the ion irradiated samples, we find that only adjusting h_K and leaving κ constant at the value of the as received samples yields a best fit between the model and the data, as seen in Fig. 1(a). In the case where we leave the h_K constant at the value of the as received samples and adjust κ , the “best fit” between the model and the data is much worse than when adjusting h_K , as also plotted in Fig. 1(a). This suggests that the reduction in h_K between the Al and substrate is much more than the reduction in κ in the probed region of the substrate due to the proton implantation. Since we probe only a small depth into the substrate at these modu-

lation frequencies, our TDTR measurements are insensitive to the damage to the crystals at the end of range. Therefore, the effects of this damage on thermal transport is much greater at the substrate surface (i.e., the interface) than in the region between the end of range and the surface. To explore this interfacial phenomenon in more detail, we plot the ion irradiated data in Fig. 1(b) with various thermal models. The best fit model using the parameters from Fig. 1(a) is included, along with model calculations when perturbing both h_K and κ by $\pm 25\%$. A change in κ of 25% causes a minimal change in the TDTR signal as compared to a 25% change in h_K . This further shows that the proton implantation has the largest effect on thermal transport on the surface of the substrate, which, after Al film evaporation, manifests itself as a decrease in the Al/substrate thermal boundary conductance.

Figure 2 shows the thermal boundary conductance at the Al/Si and Al/ Al_2O_3 interfaces as a function of proton dose. When subjected to the highest proton dose (5.79×10^{17} protons cm^{-2}), we observe an order of magnitude decrease in thermal boundary conductance in both material systems compared against the as received samples. Note that upon low doses of ion irradiation, the thermal boundary conductances exhibit a sharp decrease that does not follow the trend in dose. We irradiate the substrates before Al evaporation. Therefore, we expect the proton irradiation to only affect the substrate surface; i.e., we do not expect the irradiation to promote additional film/substrate mixing around the interface. The protons will, therefore, modify the surface, disrupting bonds and roughening the surface prior to Al evaporation. With any distribution of the energy, which would occur from any level of implantation, we expect the thermal boundary conductance to decrease by some amount ∂h_K solely based on the modification of the bonds near the surface. As the dose is increased, the physical disruption of atomic positions in the irradiation depth will increase, causing an increase in structure and surface roughness on the substrate surface prior to film deposition. Therefore, upon Al film deposition, rougher interfaces between the Al and the Si or Al_2O_3 are created with increased proton dose, F . Note, we refer to substrate roughness as not only physical variations

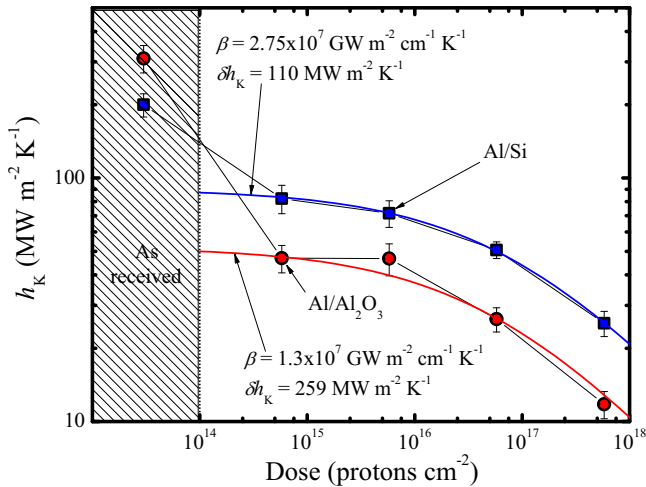


FIG. 2. (Color online) Thermal boundary conductance at the Al/Si and Al/Al₂O₃ interfaces as a function of proton dose. When subjected to the highest proton dose (5.79×10^{17} protons cm⁻²), we observe an order of magnitude decrease in thermal boundary conductance in both material systems compared against the as received samples. The sharp decreases in h_K from the as received samples to the lowest ion implanted samples is due to bond breaking from the proton irradiation, quantified as δh_K in Eq. (1). The dependence in h_K on proton dose, which is related to the atomic displacement and thereby near-surface morphology, is quantified by β . Each data point represents the average from 5 TDTR data sets taken at different locations on the sample. The standard deviation due to variations at different parts of the sample is, for the most part, smaller than the data point, representing a very small uncertainty due to differences on the sample surface. To quantify a major source of uncertainty in the measurement, we show error bars due to $\pm 5\%$ variations in Al film thickness.

on the surface but also damage of the substrate very near to the interface in a region much less than the substrate volume sampled in TDTR. Therefore, we ascribe the decrease in h_K due to ion bombardment to be due to two mechanisms: surface features (e.g., rms roughness of the substrate surface) and near-surface damage. Note that we have studied the effects of surface features on h_K at Al/Si interfaces previously,⁸ and this alone cannot explain the observed reduction in h_K due to proton implantation.

Following Gundrum *et al.*⁴ we expect the roughness at the interface to be proportional to \sqrt{F} , and therefore, the measured thermal boundary conductance as a function of proton dose is given by

$$\frac{1}{h_{K,\text{ion}}} = \frac{1}{h_{K0} - \delta h_K} + \frac{\sqrt{F}}{\beta}, \quad (1)$$

where h_{K0} is thermal boundary conductance of the as received sample and β is a constant related to the materials that are affected by the implantation.⁴ We fit Eq. (1) to the experimental data, as shown in Fig. 2. δh_K in Al₂O₃ is a factor of 2.35 larger than δh_K in Si (i.e., $\delta h_{K,\text{Al}_2\text{O}_3} / \delta h_{K,\text{Si}} = 2.35$). As we discussed, δh_K is related to tearing of the bonds at the surface of the substrate. Therefore, we expect the difference in δh_K in the two materials to be related to the differences in the bulk moduli. The bulk moduli of Al₂O₃ and Si are 240 GPa and 101.97 GPa, respectively.²⁶ The ratio of these moduli are 2.35, in remarkable agreement with $\delta h_{K,\text{Al}_2\text{O}_3} / \delta h_{K,\text{Si}} = 2.35$. This indicates that the sharp decrease in h_K at the low proton doses is due to breaking of the atomic bonds near the substrate surface from proton bombardment.

The increase in subsurface roughness and dependence of h_K on proton dose, which is quantified with β in Eq. (1), is

related to the total atomic displacement induced by the irradiation. β in Si is a factor of 2.12 higher than that in Al₂O₃ (i.e., $\beta_{\text{Si}} / \beta_{\text{Al}_2\text{O}_3} = 2.12$). Although number of displaced atoms in each substrate (dpa) is dependent on proton dose, the ratio of Si dpa Al₂O₃ dpa in our study is constant at 2.02, as previously mentioned (i.e., $\text{dpa}_{\text{Si}} / \text{dpa}_{\text{Al}_2\text{O}_3} = 2.02$). This is in excellent agreement with $\beta_{\text{Si}} / \beta_{\text{Al}_2\text{O}_3}$ determined from the experimental data in Fig. 2.

In summary, we have investigated the thermal boundary conductance across Al/Si and Al/Al₂O₃ interfaces that are subjected to varying doses of proton ion implantation. We find that even with low levels of proton doses, sharp decreases are observed in h_K due to bond breaking and reformation near the interface. Continued increase in irradiation dosage causes a continued decrease in h_K due to atomic displacement considerations. Thermal conductance at imperfect interfaces is then influenced by not only the mixing inherent with nonideal intersections but the nature of the bonds making up the boundary as well.

We are appreciative for funding from the LDRD program office through the Sandia National Laboratories. Sandia National Laboratories is a multi-program laboratory managed and operated by Sandia Corporation, a wholly owned subsidiary of Lockheed Martin Corporation, for the U.S. Department of Energy's National Nuclear Security Administration under Contract No. DEAC04-94AL85000.

¹D. G. Cahill, W. K. Ford, K. E. Goodson, G. D. Mahan, A. Majumdar, H. J. Maris, R. Merlin, and S. R. Phillpot, *J. Appl. Phys.* **93**, 793 (2003).

²E. Pop, *Nano Res.* **3**, 147 (2010).

³E. T. Swartz and R. O. Pohl, *Appl. Phys. Lett.* **51**, 2200 (1987).

⁴B. C. Gundrum, D. G. Cahill, and R. S. Averback, *Phys. Rev. B* **72**, 245426 (2005).

⁵P. E. Hopkins, P. M. Norris, R. J. Stevens, T. Beechem, and S. Graham, *J. Heat Transfer* **130**, 062402 (2008).

⁶T. E. Beechem, S. Graham, P. E. Hopkins, and P. M. Norris, *Appl. Phys. Lett.* **90**, 054104 (2007).

⁷K. C. Collins and G. Chen, *Appl. Phys. Lett.* **97**, 083102 (2010).

⁸P. E. Hopkins, L. M. Phinney, J. R. Serrano, and T. E. Beechem, *Phys. Rev. B* **82**, 085307 (2010).

⁹J. F. Ziegler, *Nucl. Instrum. Methods Phys. Res. B* **219–220**, 1027 (2004).

¹⁰M. T. Robinson, *J. Nucl. Mater.* **216**, 1 (1994).

¹¹L. W. Hobbs, J. F. W. Clinard, S. J. Zinkle, and R. C. Ewing, *J. Nucl. Mater.* **216**, 291 (1994).

¹²P. E. Hopkins, J. R. Serrano, L. M. Phinney, S. P. Kearney, T. W. Grasser, and C. T. Harris, *J. Heat Transfer* **132**, 081302 (2010).

¹³D. G. Cahill, *Rev. Sci. Instrum.* **75**, 5119 (2004).

¹⁴A. J. Schmidt, X. Chen, and G. Chen, *Rev. Sci. Instrum.* **79**, 114902 (2008).

¹⁵F. Incropera and D. P. DeWitt, *Fundamentals of Heat and Mass Transfer*, 4th ed. (Wiley, New York, 1996).

¹⁶C. Thomsen, H. T. Grahn, H. J. Maris, and J. Tauc, *Phys. Rev. B* **34**, 4129 (1986).

¹⁷C. Thomsen, J. Strait, Z. Vardeny, H. J. Maris, J. Tauc, and J. J. Hauser, *Phys. Rev. Lett.* **53**, 989 (1984).

¹⁸R. J. Stevens, A. N. Smith, and P. M. Norris, *J. Heat Transfer* **127**, 315 (2005).

¹⁹R. J. Stoner and H. J. Maris, *Phys. Rev. B* **48**, 16373 (1993).

²⁰P. E. Hopkins, R. J. Stevens, and P. M. Norris, *J. Heat Transfer* **130**, 022401 (2008).

²¹P. E. Hopkins and P. M. Norris, *Appl. Phys. Lett.* **89**, 131909 (2006).

²²E. T. Swartz and R. O. Pohl, *Rev. Mod. Phys.* **61**, 605 (1989).

²³J. C. Duda, T. Beechem, J. L. Smoyer, P. M. Norris, and P. E. Hopkins, *J. Appl. Phys.* **108**, 073515 (2010).

²⁴T. Beechem, J. C. Duda, P. E. Hopkins, and P. M. Norris, *Appl. Phys. Lett.* **97**, 061907 (2010).

²⁵P. E. Hopkins, *J. Appl. Phys.* **106**, 013528 (2009).

²⁶D. R. Lide, *CRC Handbook for Chemistry and Physics*, 89th ed. (CRC Press, Boca Raton, FL/Taylor & Francis, London, 2008).